JOURNAL OF PHYSICAL AND CHEMICAL SCIENCES

Journal homepage: http://scienceq.org/Journals/JPCS.php

Research Article Open Access

# Removal of Ni(II) Ion from Aqueous Solution using Chitosan Nanoparticles derived from Blue Crab (*Callinectes sapidus*) Shells

Ayodele Olajide[1*], Okoronkwo Afamefuna Elvis[1], Oluwasina Olugbenga Oludayo[1]

[1] Department of Chemistry, School of Sciences, The Federal University of Technology Akure, P.M.B. 704, Nigeria.

[*]Corresponding Author: Ayodele Olajide; Tel: +234 8038006203; Email: jidejahid07@yahoo.com

Received: August 11, 2017, Accepted: September 2, 2017, Published: September 2, 2017.

## ABSTRACT

Availability of drinking water is a great challenge to many communities in Nigeria. Hence, majority of rural area dwellers depend on groundwater for drinking and other purposes. This study was conducted to evaluate the effects of anthropogenic activities from petrol stations on the quality of groundwater in selected locations at Ile-Oluji, Nigeria. The samples were analysed for seven heavy metals using Atomic Absorption Spectroscopy (AAS). The statistical analysis of variance (using Tukey test) revealed no significant difference at $p<0.05$. The percent coefficients of variation for all the heavy metals analysed varied widely, except for Cd. From the foregoing results, it is evident that the groundwater located near petrol stations is unsuitable for drinking and other domestic applications. Thus, there is need for government to take urgent measures to enact and enforce appropriate legislation to regulate the locations of wells for groundwater especially in areas that are prone to anthropogenic activities.

**Keywords:** *Thermodynamics, chitosan nanoparticles, isotherms, crab shells, wastewater, adsorption,*

## INTRODUCTION

Recycling of wastewater has been considered possible as a result of advancement in science and technology [1]. The development has in good measure improved the quantity of water available for domestic, industrial, and agricultural purposes. Increased population, uncontrolled migration, industrial revolution, refuse and sewage discharge from homes and factories have played a major role in making water bodies unwholesome for use. Contamination of water by heavy metals is a global issue which poses health risk since the elements are not biodegradable [2].

Electroplating industries, ceramic industries, and other chemical industries discharge large volume of wastewater polluted with heavy metals (e.g. Pb, Zn, Cu, Ni, Cr, and Cd) into the environment [3, 4, 5, 6]. Heavy metals may bio-accumulate in living organisms through constant ingestion. Lead (Pb), when present in human body, even at low concentration damages vital organs. Body immune systems are also targeted by the toxic lead. Lead in high concentration in the body causes insomnia, persistent headache, body irritation, convulsions and seizures [7, 8]. Copper on the hand in high concentration causes anaemia. It damages various organs such as liver and kidney in human body. Over-exposure to copper causes Wilson's disease in human. The presence of copper in aquatic habitats is poisonous to aquatic organisms living in them [9, 10].

Various processes such as coagulation-flocculation [11, 12], membrane-filtration [13], and oxidation [14, 15] have been employed to remove organic pollutants from wastewaters. However, Ion exchange, electro-coagulation, and electrolytic reduction processes have been employed for the removal of heavy metals in wastewater. Adsorption process is now popular as an effective method of removing heavy metals [16, 17, 18].

Chitosan due to its exceptional chelating ability appears to be a potent adsorbent [19]. It is a copolymer of glucosamine and N-acetyl glucosamine units [20] which can be obtained by de-acetylating chitin. Chitosan structure closely resembles the structure of cellulose, except that the hydroxyl group at $C_2$ position in cellulose is replaced by amino group. Chitosan exhibits antibacterial, antifungal, and antiviral properties. It can be made into film, fibre, and hydrogel [21, 22]. Chitosan finds applications in medical field, it has been extensively used in cosmetic, food, pulp and paper, and textile industries [23, 24]. Chitosan is good for producing metal complexes as effective protein coagulants [25].

Chitosan nanoparticle was chosen for this research work because of the large surface area to volume ratio inherent from the reduction of particle size. The reduction in the particle size would expose several active sites on the adsorbent surface, which will invariably improve the efficiency of the adsorbent to remove Ni(II) ion from aqueous solution.

## METHODOLOGY

### Materials

Sodium tripolyphosphtae (TPP), hydrochloric acid (HCl), sodium hydroxide (NaOH) pellets, acetic acid, and hydrated $NiSO_4.6H_2O$ used in this research were of analytical grade, purchased from Sigma Aldrich Chemical Company. Blue crab shells were collected from a local market in Lagos, Nigeria.

### Adsorbent preparation

Blue crab shells were dried and ground into powder. The powder was demineralised using 0.7 M HCl (at 65ºC for 3 h) and washed severally with distilled water. The protein content of the sample was removed using 1.2 M NaOH (at 65ºC for 30 min). The resulting sample was washed to neutrality using distilled water to obtain chitin. Chitosan was obtained by de-acetylating chitin with 50% NaOH (at 100ºC for 3 h), washed and dried at 65ºC. The resulting product was converted to chitosan nanoparticles by dissolving in 1 M acetic acid. The mixture was filtered and the nanomaterial was precipitated the by addition of sodium tripolyphosphate (TPP) in a drop-wise manner. The chitosan nanoparticles were washed with distilled water and filtered using sinter glass (size G-3). The final product was characterised using Scanning Electron Microscopy (SEM), X-Ray Diffraction (XRD) and Fourier Transform Infra-Red (FTIR).

**Batch adsorption process**

Adsorption process was carried out using chitosan nanoparticles as adsorbent for the removal of Ni(II) ion from aqueous solution. 50 mg/L of metal solution was prepared from the stock solution (1000 mg/L), 50 mL was measured into conical flasks and the pH was adjusted appropriately. 0.5 g of the adsorbent was added to each beaker, the mixture was agitated at regular interval for 6 h, filtered and analysed using Atomic Absorption Spectrophotometer (AAS Buck Scientific 210). Point of zero charge was investigated by dissolving 0.1 g of the adsorbent in 50 mL 0.1 M $KNO_3$ as variation in pH was recorded after 24 h. Contact time and concentration studies were carried out simultaneously using the optimum pH. Effect of temperature variation (room temp, 35, 45, 55, and 65 $^oC$) was investigated using the optimal pH and time. The amount of uptake by metal ion was calculated using equation 1.

$$q_e = \frac{(C_o - C_e)V}{m} \quad (1)$$

Where $q_e$ (mg/g) is the quantity of metal ion uptake, $C_o$ (mg/L) is the initial metal ion concentration, $C_e$ (mg/L) is the non-adsorbed molecules left in the adsorbate, V (mL) is the volume of metal ion solution, and m (g) is the mass of the adsorbent.

Percentage uptake was calculated using equation 2.

$$\text{Metal removal } (\%) = \frac{(C_0 - C_e)}{C_e} \times 100 \quad (2)$$

## RESULTS AND DISCUSSION

**FTIR, XRD and SEM analyses of chitosan nanoparticles**

The chitosan nanoparticles were characterised using Fourier Transform Infra-red, Scanning Electron Microscopy (SEM), and X-Ray Diffraction as presented in Fig. 1, 2 and 3, respectively. The following peaks were observed from the FTIR spectrum: 3447.87 $cm^{-1}$, representing O-H stretch of alcoholic and phenolic groups; 2931.90 $cm^{-1}$, denoting C-H stretch, 1643.41, 1435.09 and 873.78 $cm^{-1}$, representing N-H bend, C-C stretch (in ring) and N-H wag of primary and secondary amines respectively; and 1050.28 $cm^{-1}$, denoting C-O stretch of alcohols. The scanning electron micrograph of chitosan nanoparticles is presented in Fig. 2. The image shows the nature of the surface of the adsorbent, the particles appear distinct and form a cluster of many fine particles. The scale of the micrograph was 20 µm. Fig. 3 shows the XRD image of chitosan nanoparticles. The two major peaks of chitosan often appear at 2Θ = 10° and 20°. However, the peak at 2Θ = 10° shifted forward to 13° while the peak at 2Θ = 20° did not shift. The shifting in the angle could be due to the fact that the chitosan in its pure form has been chemically modified using TPP to give chitosan nanoparticles.

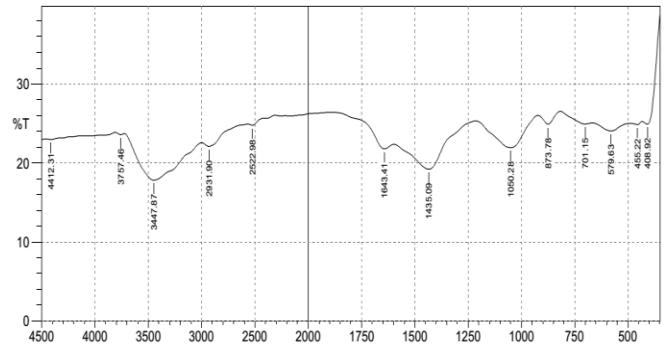


Figure 1: FTIR spectrum of chitosan nanoparticles

The chemical conversion caused other conspicuous peaks to show on the XRD image (Fig. 3). The particle size of the chitosan nanoparticles was 9.94 nm.

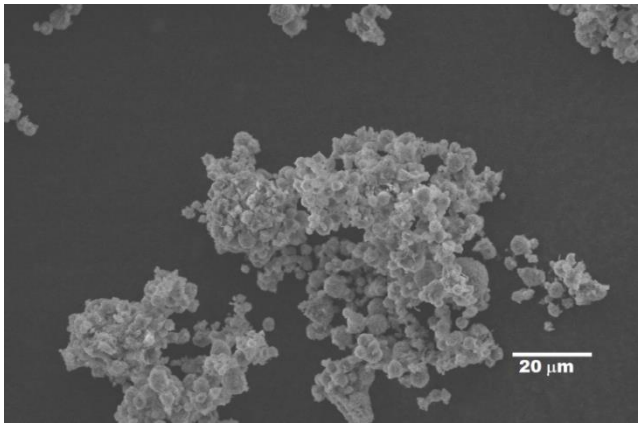


Figure 2: SEM image of chitosan nanoparticles

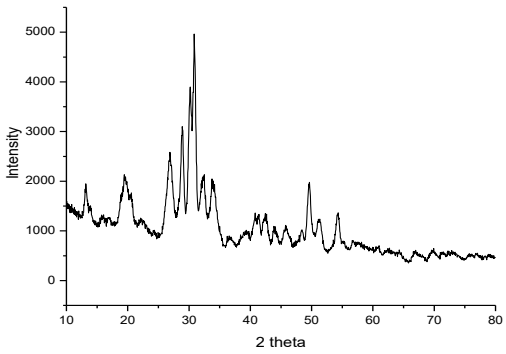


Figure 3: X-Ray Diffractogram chitosan nanoparticles

**pH studies and point of zero charge (pzc)**

Effect of pH on the removal process of Ni(II) ions was presented in Fig. 4. It was observed that there was a slow removal of metal ion at low pH which later progressed considerably as the pH increased. The low removal of metal ions at low pH could be as a result of an increased competition between the species in the adsorbate and protons. Zamil *et al.* [26] reported that increase in pH leads to increase in total number of negative groups available for the binding of metal ions which invariably leads to reduced competition between proton and metal ions. From the results, it was observed that Ni(II) ion removal peaked at pH 6. Godea *et al.* [27] reported that Ni(II) ion forms a precipitate at pH greater than 8; and Kurniawan *et al.* [28] reported that precipitate of $Cu(OH)_2$ tends to be formed at pH>6.

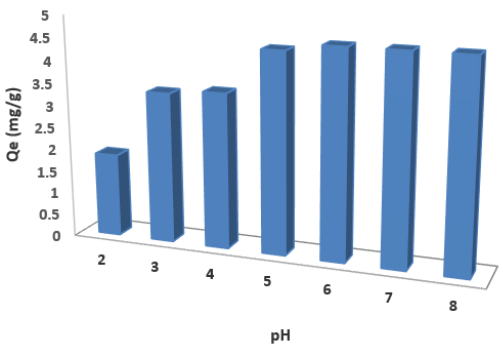


Figure 4: Effects of pH on Ni(II) ion removal

The point of zero charge of any adsorbent is the pH in which the net charge at the surface of the adsorbent is zero [29]. Fig. 5 shows that the point of zero charge of chitosan nanoparticles occurred at pH 6.3. At this point, the magnitude of the positive charge at the surface were at equilibrium with the negative charge at the surface of the adsorbent.

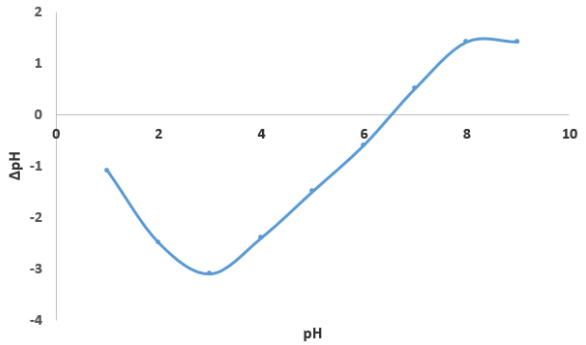


Figure 5: The point of zero charge of chitosan nanoparticles

Fiol and Villaescusa [29] reported that if the pH of the solution is higher than the point of zero charge, then the surface charge of the solid adsorbent will be negative which can then attract metal ions (cations). Also, if the pH of point of zero charge is higher than the pH of the solution, the adsorbent surface charge therefore becomes positive, and this will thereby draw negative ions onto the surface. Adsorptive system is therefore a competitive process between hydrogen/hydroxyl ions and the adsorbate species, in which negatively charged species are better adsorbed at lower pH and positively charged species are better adsorbed at higher pH.

**Contact time and kinetic studies at different concentration**

Effects of time variation on the removal of Ni(II) ion from aqueous solution were studied alongside concentration as presented in Fig. 6. It was observed that increase in time favoured the uptake of nickel ion, this was as a result of many active sites that were readily available for metal binding. The number of active sites is most likely to reduce as the metal ions continue to adhere to the adsorbent pores. In Fig. 6, there was a rapid uptake of metal ion at the initial stage which increased considerably and peaked at 120 min for the different concentrations under study. A slight decrease occurred after optimum time (120 min), this could be as a result of further agitation which could render some of the adsorbed species mobile, and thus return into the solution.

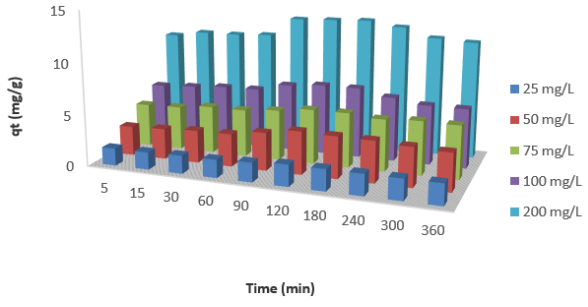


Figure 6: Contact time studies for the uptake of Ni(II) ion at different concentrations

The data obtained from the contact time studies with varied concentrations were evaluated using kinetic models (pseudo-first order and pseudo-second order).

Lagergren [30] expressed pseudo-first order kinetic model as;

$$\frac{dq}{dt} = kad(qe - qt) \qquad (3)$$

Where $q_e$ (mg/g) is the metal ion uptake at equilibrium, $q_t$ (mg/g) is the metal ion uptake at time $t$, and $k_{ad}$ (L/min) represents first order rate constant. Equation 3 was integrated (using boundary conditions: $t$ = 0 to $t$ and $q$ = 0 to $qe$) to give a linear expression (equation 4).

$$Log\ (q_e - q_t) = logq_e - \frac{kad}{2.303}t \qquad (4)$$

Log ($q_e$-$q_t$) was plotted against t (min) for the removal process of Ni(II) ion as presented in Fig. 7. The values of $q_e$ and $k_{ad}$ were extrapolated from the intercept and the slope of the plot respectively, and the results are presented in Table 1.

Pseudo-second order kinetic model is expressed in equation 5;

$$\frac{t}{q} = \frac{1}{k_{2,q^2e}} + \frac{1}{q_e}t \qquad (5)$$

Where $q_e$ (mg/g) and $k_2$ (g $mg^{-1}min^{-1}$) are the metal ion uptake at equilibrium and pseudo-second order rake constant. t/q (min/mg g) was plotted against t (min) as presented in Fig. 8, the values of $q_e$ and $k_2$ were estimated from the slope and the intercept, respectively. Table 1 shows the parameters of pseudo-first order and pseudo-second order kinetic models. It was observed that the correlation coefficient $R^2$ for pseudo-second order model approached unity unlike $R^2$ of pseudo-first order that was not tending to one. Comparing the experimental $q_{e\ Exp}$ (mg/g) and the estimated $q_{e\ Est}$ (mg/g) of pseudo-first order and pseudo-second order kinetic models, it was observed that $q_{e\ exp}$ and $qe_{\ Est.}$ values for pseudo-second order were close to each other, whereas, there was a wide margin between values of $q_{e\ exp}$ and $q_{e\ Est}$ for pseudo-first order kinetic model, the implication is that, pseudo-second order kinetic model was more suited than pseudo-second order kinetic model. Reports have suggested that most adsorption processes are always in consonance with pseudo-second order kinetic model [31, 32].

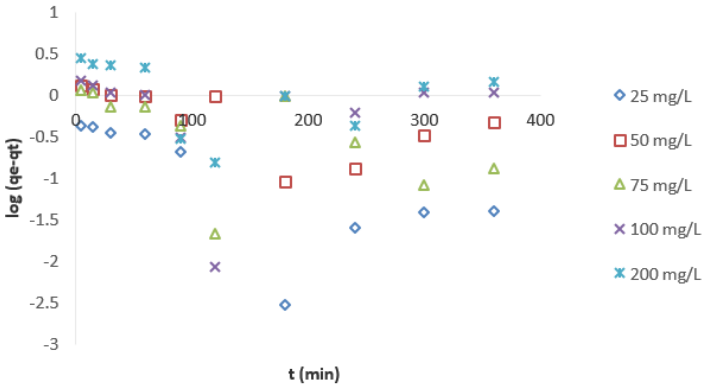


Figure 7: Pseudo-first order kinetic plot for Ni(II) ion removal

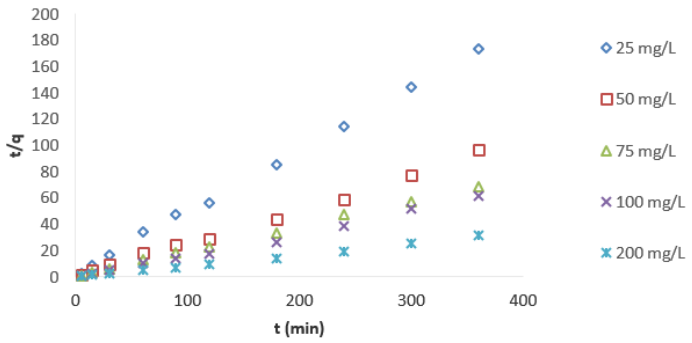


Figure 8: Pseudo-second order kinetic plot for Ni(II) ion removal

Table 1: Kinetic parameters for the removal of Ni(II) ion

| Pseudo-first order | | | | | Pseud-second order | | |
|---|---|---|---|---|---|---|---|
| $C_o$ (mg/L) | $Q_{e\ Exp.}$ (mg/g) | $Q_{e\ Est.}$ (mg/g) | $K_1$ ($min^{-1}$) | $R^2$ | $Q_{e\ Est.}$ (mg/g) | $K_2$ ($gmg^{-1}$) | $R^2$ |
| 25 | 2.114 | 0.443 | 0.009 | 0.431 | 2.114 | 0.097 | 0.999 |
| 50 | 4.194 | 1.027 | 0.005 | 0.404 | 3.896 | 0.109 | 0.995 |
| 75 | 5.343 | 0.761 | 0.006 | 0.306 | 5.277 | 0.052 | 0.999 |
| 100 | 6.882 | 0.561 | -0.002 | 0.003 | 5.893 | -0.031 | 0.993 |
| 200 | 12.893 | 1.338 | 0.002 | 0.055 | 11.728 | -0.039 | 0.995 |

Initial metal ion concentration and isotherm studies

Initial metal ion concentrations were varied with time for the removal process of Ni(II) ion. It was observed that increase in the initial metal ion concentration did not favour metal removal as there was a decrease in the uptake, this could be due to an increase in adsorbate concentration without corresponding increase in the adsorbent dosage. Futalan *et al.* [33] and Kamari and Ngah [34] reported that, a number of adsorption active sites were readily available at the start, as a result of this, metal ion uptake would be rapid, before slowly attaining an equilibrium. Cybelle *et al.* [35] reported that when adsorption process approaches equilibrium, active sites on the surface are almost filled up with metal ions. The unfilled sites on the surface will not be readily available anymore, and become more difficult for metal ions to adhere onto the sites because of repulsion forces at the interface.

The generated data from concentration studies were subjected to Langmuir, Freundlich, Temkin and Dubinin-Radushkevich models. Langmuir isotherm is a widely used expression for metal ion uptake in adsorption process as it assumes that a particular adsorbent has a definite amount of active sites with the same energy level for monolayer coverage [36].

Langmuir model is given in equation 6;

$$\frac{C_e}{q_e} = \frac{1}{bq_m} + \frac{C_e}{q_m} \quad (6)$$

Where $q_m$ ($mgg^{-1}$) and b ($mLmg^{-1}$) are the maximum adsorption capacity for monolayer coverage and Langmuir constant for the association of adsorbate species onto the active sites [37]. Fig. 9 shows the Langmuir plots for Ni(II) ion removal. The values of $q_m$ and b (Table 2) were extrapolated from the intercepts and the slopes, respectively. Correlation coefficient $R^2$ did not tend to one which implies that Langmuir model was not in totality obeyed. Another important parameter that dictates the favourability of Langmuir isotherm model is $R_L$ (equation 7), a separation factor which can be deduced from Langmuir expression;

$$R_L = \frac{1}{1+bC_o} \quad (7)$$

Where b and $C_o$ represent constant of Langmuir adsorption equilibrium (mL/mg) and initial metal ion concentration (mg/L). When $R_L = 0$, it is an irreversible process; favourable when $0<R_L<1$; unfavourable when $R_L>1$; and linear when $R_L = 1$. In Table 2, the values of $R_L$ at different time interval were less than 1 but greater than 0 which implied favourable adsorption process in the removal of the metal ions.

Freundlich model (equation 8) is based on the assumption of reversible adsorption of heterogeneous systems [34].

$$logq_e = logK_F + \frac{1}{n_F} logC_e \quad (8)$$

Where $k_F$ ($mgg^{-1}$) is the Freundlich adsorption capacity; and $1/n_F$ represents Freundlich heterogeneity factor also denoted as $b_F$. The parameter, $b_F$ describes the intensity of adsorption on the heterogeneity of the surface. The solid phase becomes more heterogeneous when $b_F$ tends to zero [39]. Fig. 10 shows the Freundlich plot of Ni(II) ion removal process. Freundlich constants; $k_F$ and $b_F$ were estimated from the intercept and slope, respectively, and the values are presented in Table 2. Correlation coefficient ($R^2$) for the removal of Ni(II) ion tended to one, suggesting that the data fitted well into Freundlich model which implies heterogeneous system. The heterogeneity of the system is established when the value of $1/n_F$ falls between zero and one, suggesting a strong bond between metal ion and adsorbent [40].

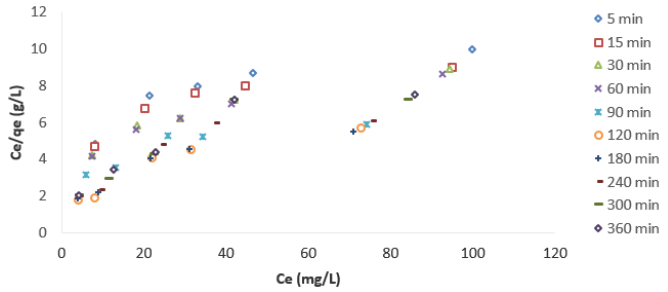


Figure 9: Langmuir plots of Ni(II) ion removal at different time interval

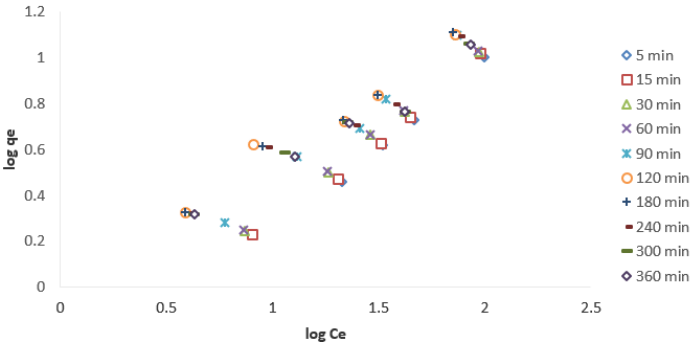


Figure 10: Freundlich plots of Ni(II) ion removal at different time interval

Temkin [41] gave a linear expression for the energy involved in adsorption process due to the relationship among the interacting entities. Temkin model points to the evenly distribution of the energies available for binding in all the active sites. Temkin model (equation 9) is often applied in its linear form [42] (Temkin and Phoyez, 1940).

$$q_e = BlnA + BlnC_e \quad (9)$$

$$B = \frac{RT}{b} \quad (10)$$

Where A (L/g) is Temkin isotherm constant, b (J/mol) is a constant related to heat energy available in sorption, R is gas constant (8.314 J/molK), and T (K) is the absolute temperature. The quantity of uptake, qe (mg/g) was plotted against lnCe and the results are

presented in Fig. 11. The $R^2$ values at different time interval showed some levels of conformity to Temkin model as presented in Table 2.

Table 2**:** Isotherm parameters for the removal of Ni(II) ion

| | Langmuir parameters | | | | | Frieundlich parameters | | | Temkin parameters | | |
|---|---|---|---|---|---|---|---|---|---|---|---|
| Time (min) | $Q_{max}$ (mg/g) | b | $R_L$ | $K_L$ ($dm^3$/g) | $R^2$ | $K_F$ ($dm^3$/g) | $1/n_F$ or $b_F$ | $R^2$ | A | B | $R^2$ |
| 5 | 21.277 | 0.008 | 0.712 | 0.172 | 0.767 | 0.351 | 0.715 | 0.990 | 0.146 | 7.432 | 0.871 |
| 15 | 24.096 | 0.007 | 0.730 | 0.179 | 0.747 | 0.341 | 0.740 | 0.993 | 0.144 | 7.952 | 0.869 |
| 30 | 20.325 | 0.010 | 0.652 | 0.217 | 0.906 | 0.419 | 0.707 | 0.999 | 0.167 | 7.816 | 0.909 |
| 60 | 21.186 | 0.010 | 0.658 | 0.219 | 0.900 | 0.417 | 0.714 | 0.999 | 0.167 | 7.988 | 0.906 |
| 90 | 26.110 | 0.011 | 0.643 | 0.291 | 0.740 | 0.599 | 0.595 | 0.980 | 0.201 | 9.205 | 0.871 |
| 120 | 17.762 | 0.027 | 0.424 | 0.484 | 0.832 | 1.069 | 0.561 | 0.960 | 0.395 | 7.495 | 0.868 |
| 180 | 18.762 | 0.025 | 0.448 | 0.462 | 0.826 | 0.987 | 0.585 | 0.976 | 0.360 | 7.821 | 0.868 |
| 240 | 17.036 | 0.024 | 0.455 | 0.408 | 0.726 | 0.994 | 0.551 | 0.946 | 0.362 | 7.103 | 0.811 |
| 300 | 15.060 | 0.026 | 0.436 | 0.390 | 0.779 | 0.980 | 0.532 | 0.960 | 0.362 | 6.536 | 0.836 |
| 360 | 15.267 | 0.024 | 0.456 | 0.367 | 0.794 | 0.934 | 0.537 | 0.970 | 0.344 | 6.504 | 0.840 |

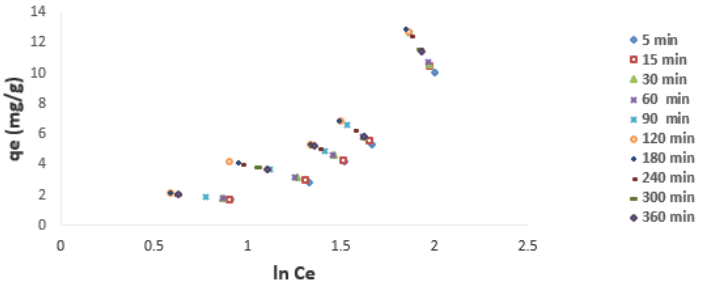


Figure 11: Temkin plots of Ni(II) ion removal at different time interval

Dubinin–Radushkevish (D-R) isotherm as described by Horsfall *et al.* [43] is expressed in equation 11, its linearized form is presented in equation 12:

$$q_e = q_D \exp(-B_D[RTln\left(1+\frac{1}{C_{eq}}\right)]^2) \qquad (11)$$

$$lnq_e = lnq_D - 2B_D RTln(1+\frac{1}{C_e}) \qquad (12)$$

Where $B_D$ and $q_D$ are the sorption free energy per mole of the adsorbate and the constant of Dubinin-Radushkevich isotherm for the surface of the adsorbent, respectively. R is gas constant (8.314 $Jmol^{-1}K^{-1}$) and T is temperature in Kelvin. Correlation coefficient ($R^2$) for Ni(II) ion removal was 0.8447 indicating some level of conformity to D-R model. The value of sorption free energy ($B_D$) was $6\times10^{-7}$ $J^2mol^{-1}$, while the Value of $q_D$ was 2.431 mg/g which denoted good adsorption capacity. Igwe and Abia [44] reported that the higher the value of $q_D$, the higher the adsorption capacity within the system.

The energy, E involved in the removal process is expressed in equation (13).

$$E = \frac{1}{(2B_D)^{\frac{1}{2}}} \qquad (13)$$

The energy (E) often times predicts the type of adsorption process. In this study, the value of E was 0.9130 kJ/mol which was well below 8 $kJmol^{-1}$, implying physical adsorption.

**Thermodynamic studies**

Thermodynamic parameters for the removal process of Ni(II) ion were estimated using vant' Hoff expression (equation 14).

$$lnK_d = \frac{\Delta S}{R} - \frac{\Delta H}{RT} \qquad (14)$$

ΔH and ΔS are the enthalpy and entropy changes, respectively. The parameters were calculated from the slope and the intercept of $lnk_d$ plotted against 1/T. R is gas constant (8.314 kJ/molK), T is temperature in Kelvin, and $K_d$ is the thermodynamic constant.

Gibb's free energy is expressed in equation 15;

$$\Delta G = -RTlnK_d \qquad (15)$$

Where ΔG is the change in Gibb's free energy of sorption process, R is gas constant (8.314 kJ/molK), T is temperature in Kelvin, and $k_d$ is the thermodynamic constant of equilibrium.

The thermodynamic studies showed that ΔS was negative (-122.590 $Jmol^{-1}K^{-1}$) which implied association between the adsorbate and the adsorbent, the negative value also offered minimum restriction for the adherence of the adsorbate onto the adsorbent active sites. ΔH value was negative (-40.5291 $kJmol^{-1}$) which indicated exothermic reaction. The values of ΔG at 301, 308, 318, 328 and 338 K were negative; having -4.1680, -2.8544, -3.4950, -2.1828, and -2.2492 $kJmol^{-1}K^{-1}$, respectively. This implied that the adsorption process was feasible and spontaneous.

## CONCLUSION

Crabs shells are underutilised materials which often times constitute nuisance to the environment when disposed indiscriminately. Although the shells are waste materials from crabs, but they can still be harnessed to produce chitosan (a natural polymer), which could be very useful for wastewater treatment. The efficacy of chitosan nanoparticles to remove heavy metals from aqueous solution has been investigated in this research. The kinetics of the process showed that the data fitted well into pseudo-second order kinetic model, while the isotherm studies showed that the data generated fitted well into Freundlich isotherm. The thermodynamic studies revealed that exothermic energy was involved, while negative ΔG meant that the process was feasible and spontaneous.

## REFERENCES


1. A. Sonune, R. Ghate, Developments in wastewater treatment methods, Desal. 167(2004) 55–63.
2. G. Crini, Recent Developments in Polysaccharide–Base Materials used as adsorbents in Wastewater Treatment, Progress in Polymer Science. 30 (2005) 38–70.
3. S. E. Bailey, T. J. Olin, R. M. Brick, D. D. Adrian, A review of potentially low cost sorbents for heavy metals. Water Research, 33 (1999) 2469 – 2479.

4. M. Ajmal, R. A. K. Rao, J. A. Anwar, R. Ahmad, Adsorption studies on rice husk: removal and recovery of Cd(II) from wastewater, Bioresource Technology. 86 (2003) 147-149.
5. M. E.Argun, S. Dursun, A new approach to modification of natural adsorbent for heavy metal adsorption, Bioresource Technology. 99(7) (2008) 2516 – 2527.
6. O. E. A. Salam, A. N. Reiad, M. M. ElShafei, A study of removal characteristics of heavy metals from wastewater by low-cost adsorbents. Journal of Advanced Research. 2 (2011) 297–303.
7. R. A.Wuana, F. E. Okieimen, Heavy Metals in Contaminated Soils: A Review of Sources, Chemistry, Risks and Best Available Strategies for Remediation, ISRN Technology (2011).
8. N. Zahra, Lead Removal from Water by Low Cost Adsorbents: A Review, *Pakistan* Journal of Analytical and Environmental Chemistry. 13(1) (2012) 1–8.
9. C. S. S. K. Gamakaranage, C. Rodrigo, S. Weerasinghe, A. Gnanathasan, V. Puvanaraj, H. Fernando, Complications and management of acute copper sulphate poisoning; a case discussion, Journal of Occupational Medicine and Toxicology (London, England), 6(1), (2011) 34-41.
10. L. E. Fazzio, G. A Mattioli, E. F. Costa, S. J. Picco, D. E. Rosa, J. A. Testa, E. J. Gimeno,. Renal cortex copper concentration in acute copper poisoning in calves, Pesquisa Veterinária Brasileira, 32(1) (2012) 1-4.
11. D. Bromley, M. Gamal, D. W. Smith, A low cost treatment process to reduce phosphorus and suspended solids in liquid wastes from animal farm operations. Proc. 4th international livestock waste manage. Symp. Technol. Expo. Malaysia society of animal production, penang, Malaysis 215 (2002).
12. O. S. Amuda, I. A. Amoo, O. O. Ajayi, Performance optimization of coagulation/flocculation process in the treatment of beverage industrial wastewater. Journal of Hazardous Materials. 129 (2006) 69-72.
13. I. I. Galambos, J. M. Molina, P. Jaray, G. Vatai, E. Bekassy–Molnar, High organic content industrial wastewater treatment by membrane filtration, Desalination. 162 (2004) 117-120.
14. N. S. S. Martinez, J. F. Fernandez, X. F. Segura, A. S. Ferrer, Preoxidation of an extremely polluted industrial wastewater by the Fenton's reagent. J. Haz. Mat. B101 (2003) 315-322.
15. J. A. Peres, J. Beltran de Heredia, J. R. Dominguez, Integrated Fenton's reagent - coagulation/ flocculation process for the treatment of cork processing wastewaters. Journal of Hazardous Materials. 107 (2004) 115-121.
16. J. Z. Xie, H. L. Chang, J. J. Kilbane, Removal and recovery of metal ions from wastewater using biosorbents and chemically modified biosorbents. Bioresource Technology, 57(2) (1996) 127-136.
17. H. Eisazadeh, Removal of chromium from waste water using polyaniline, Journal of Applied Polymer Science. 104(3) **(**2007) 1964-1967.
18. C. G. Rocha, D. A. M. Zaia, R. V. S.Alfaya, A. A. S. Alfaya, Use of rice straw as biosorbent for removal of Cu (II), Zn (II), Cd (II) and Hg (II) ions in industrial effluents. Journal of Hazardous Materials. 166(1) (2009) 383-388.
19. M. N. V. Ravi-Kumar, A review of chitin and chitosan applications React. *Funct. Polym*. 46, (2000) 1-27.
20. D. P. Chattopadhyay, S. I. Milind, Aqueous Behaviour of Chitosan. *Hindawi Publishing Corporation International Journal of Polymer Science* 7 (2010).
21. R. A. A. Muzzarelli, Chitin chemistry, in The Polymeric Materials Encyclopedia. Salamone JC, Ed. 312–314, CRC Press, Boca Raton Fla, USA (1996).
22. S. Hirano, ULLMANN's Encyclopedia of Industrial Chemistry; 7 Wiley-VCH, Weinheim, Germany, 6th edition (2003).
23. P. K. Dutta, J. Duta, V. S. Tripathi, Chitin and Chitosan: chemistry, properties and applications, Journal of Scientific and Industrial Research. 63(1) (2004) 20–31.
24. K. V. Harish-Prashanth, R. N. Tharanathan, Chitin/chitosan: modifications and their unlimited application potential-an overview, Trends in Food Science and Technology. 18(3) (2007) 117–131.
25. G. Ashoka, S. Fereidoon, Use of chitosan for the removal of metal ion contaminants and proteins from water. Environmental Science Program, Department of Biochemistry, Memorial University of Newfoundland, St. John's, NL; Canada A1B 3X9 (2007).
26. S. S. Zamil, S. Ahmad, M. H. Choi, J. Y. Park, S. C. Yoon,. Correlating metal ionic characteristics with biosorption capacity of Staphylococcus saprophyticus BMSZ711 using QICAR model, Bio-resource Techn. 100 (2009) 1895–1902.
27. F. Godea, E. D. Atalay, E. Pehlivan,. Removal of Cr(VI) from Aqueous Solutions using Modified Red Pine Sawdust, Journal of Hazard. Mat. 152 (2008) 1201–1207.
28. T. A. Kurniawan, G. Y. S. Chan, W. H. Lo, S. Babel, Comparisons of low-cost adsorbents for treating wastewaters laden with heavy metals, Journal Science of the Total Environment, 36 (2006) 409–426.
29. N. Fiol, I. Villaescusa, Determination of sorbent point zero charge: usefulness in sorption studies, Environmental Chemistry Letters, 2008.
30. S. Lagergren, About the theory of so-called adsorption of soluble substances. K. Sven. Vetenskapsakad. Handlingar Band 24(1898) 1-39.
31. Y. S. Ho, G. McKay, D. A. J. Wase, C. F. Foster, Study of the sorption of divalent metal ions onto peat. *Adsorp. Sci. Technol*. 18(2000) 639–650.
32. N. T. Abdel-Ghani, A. K. Hegazy, G. A. El-Chaghaby, Typha domingensis leaf powder for decontamination of aluminium, iron, zinc and lead: Biosorption kinetics and equilibrium modelling, International Journal of Environmental Science and Technology, 6(2) (2009) 243-248.
33. C. M. Futalan, C. C. Kan, M. L. Dalida, K. J. Hsien, C. Pascua, M. W. Wan, Comparative and competitive adsorption of copper, lead, and nickel using chitosan immobilized on bentonite. Carbohyd. Polym. 83(2) (2011) 528-536.
34. A. Kamari, W. S. W. Ngah, Isotherm, kinetic and thermodynamic studies of lead and copper uptake by $H_2SO_4$ modified chitosan. *Colloid Surf. B*. 73(2) (2009) 257-266.
35. M. F. Cybelle, T. Wan-Chi, L. Shiow-Shyung, L. D. Maria, W. Meng-Wei, Copper, nickel and lead adsorption from aqueous solution using chitosan-immobilized on bentonite in a ternary system. *Sustain. Environ. Res*. 22(6) (2012) 345-355.
36. J. Febrianto, A. N. Kosasih, J. Sunarso, Y. H. Ju, N. Indraswati, S. Ismadji, Equilibrium and kinetic studies in adsorption of heavy metals using biosorbent: A summary of recent studies, Journal of Hazardous Mat. 162(2-3) (2009) 616-645.
37. Y. Vijaya, S. R. Popuri, V. M. Boddu, A. Krishnaiah, Modified chitosan and calciumalginate biopolymer sorbents for removal of nickel (II) through adsorption. *Carbohydrate Polymer* 72(2) (2008) 261-271.

38. F. Haghsherest, G. Lu, Adsorption characteristics of phenolic compounds onto coal-reject-derived adsorbent. *Energ. Fuel*. 12(6) (1998) 1100-1107.
39. V. O. Arief, K. Trilestari, J. Sunarso, N. Indraswati, S. Ismadji,. Recent Progress on Biosorption of Heavy Metals from Liquids Using Low Cost Biosorbents: Characterization, Bios. Parameters and Mech. Studies, Clean. 36(12) (2008) 937-962.
40. M. I. Temkin, Adsorption equilibrium and process kinetics on homogenous surfaces and with interaction between adsorbed mol. Zh. Fiz. Khim, 15(3) (1941) 296-332.
41. M. I. Temkin, V. Phoyez, Kinetics of ammonia synthesis on promoted iron catalysts. *Acta Physicochim*, URSS 12 (1940)327-352.
42. M. Horsfall (Jnr), A. L Spiff, A. A. Abia, *Bull. Korean Chem. Soc*. 25(7) (2004) 969-976.
43. J. C. Igwe, A. A. Abia, Adsorption isotherm studies of Cd (II), Pb (II) and Zn (II) ions bioremediation from aqueous solution using unmodified and EDTA-modified maize cob 32(1) (2007) 33-42.

**Citation:** Ayodele Olajide *et al*. (2017). Removal of Ni(II) Ion from Aqueous Solution using Chitosan Nanoparticles derived from Blue Crab (*Callinectes sapidus*) Shells. j. of Physical and Chemical Sciences.V5I4. DOI: 10.15297/JPCS.V5I4.01

**Copyright:** © 2017 Ayodele Olajide, This is an open-access article distributed under the terms of the Creative Commons Attribution License, which permits unrestricted use, distribution, and reproduction in any medium, provided the original author and source are credited.